Stability of Relativistic Blast Waves

Jun Ogura[*) and Yasufumi Kojima[**)

Department of Physics, Hiroshima University, Hiroshima 739–8526, Japan

A spherical blast wave with relativistic velocity can be described by a similarity solution, that is used for theoretical models of gamma-ray bursts. We consider the linear stability of such a relativistic blast wave propagating into a medium with density gradient. The perturbation can also be expressed by a self-similar form. We show that the shock front is unstable in general, and we evaluate the growth rate.

§1. Introduction

Gamma-ray bursts have puzzled astronomers since their accidental discovery in the late sixties. Recent observations still provide new topics of study, afterglow, [1] optical flash, [2] brightest events, [3] and so forth. In these bursts, huge amounts of energy are released instantaneously. The subsequent evolution of the radiation-dominated matter can be described by an expanding blast wave. Gamma-rays are emitted when a matter with highly relativistic velocity, with Lorentz factor $\Gamma \geq 10^2$, is converted into radiation.

The observed fluctuations in gamma-rays with a short timescale are thought to be associated with the complex behavior of shock waves. Two locations have been proposed as the origin of the irregularities. One location is inside the relativistic fluid, as described by the internal shock model. When shock waves intersect each other, gamma-rays are emitted. The complexity of the corresponding time profile depends on the internal shock structure. The other location is in the shock front itself, as described by the external shock model. When the shock front impinges upon ISM (inter stellar matter), gamma-rays are emitted. Both models have advantages and disadvantages. Waxman [4) 5)] showed synchrotron emission from external shocks provides a successful model for the broken power law spectra and smooth temporal behavior of afterglow. Sari and Piran, [6] however, showed that external shocks cannot produce variable gamma-ray bursts unless they are produced by extremely narrow jets or if only a small fraction of the shell emits radiation. The expanding shell and ISM were assumed to be smooth. The observed nature with rapid variability depends on the fluctuations of the external matter, which is not yet known. The possibility of irregularity in the shock front can be investigated. An irregular shell with angular fluctuations in the external shock may produce temporal behavior of the gamma-ray emission.

A theoretical model of the blast wave with ultra-relativistic speed was considered

---

[*) E-mail: ogura@theo.phys.sci.hiroshima-u.ac.jp
[**) E-mail: kojima@theo.phys.sci.hiroshima-u.ac.jp

by Blandford and McKee.[7] They obtained a spherical self-similar solution, which can be regarded as the relativistic version of the Sedov-Taylor solution. Using a numerical code for the spherical symmetry, Kobayashi, Piran and Sari[8] simulated an expanding shock with relativistic speed and confirmed that the self-similar solution is a good approximation. The spherical symmetry may be too great a simplification in some cases. Indeed, in non-relativistic hydrodynamics, Ryu and Vishniac[9] showed that under certain conditions the spherical shock becomes overstable with respect to perturbations with tangential velocity. From this point of view, it is important to examine the dynamical stability of the Blandford-McKee solution.

In this paper, we consider the linear stability with respect to non-spherical deformations of ultra-relativistic shock waves. There is a similarity solution describing shocks with an impulsive energy supply. In Section 2, we show that the perturbation functions can be obtained in a power low form. Matching the boundary conditions at the shock front and using a regularity condition at the origin, the temporal behavior, i.e. an eigenvalue of the functions, is determined. Section 3 is devoted to discussion.

§2. Basic equations and approximate solutions

2.1. *Sphrical shock waves*

Relativistic fluid motion is described by conservation laws of number and energy-momentum. We explicitly give these equations in spherical coordinates for two-dimensional flow with the velocity (v_r, v_θ) and the Lorentz factor γ as

$$\partial_t D + \frac{1}{r^2}\, \partial_r\,(r^2\, D\, v_r) + \frac{1}{r\,\sin\theta}\partial_\theta\,(\sin\theta\, D\, v_\theta) = 0, \quad (2\cdot1\text{a})$$

$$\partial_t\,(W - p) + \frac{1}{r^2}\,\partial_r\,(r^2\, W\, v_r) + \frac{1}{r\,\sin\theta}\,\partial_\theta\,(\sin\theta\, W\, v_\theta) = 0, \quad (2\cdot1\text{b})$$

$$\partial_t\,(W\, v_r) + \frac{1}{r^2}\,\partial_r\,\{r^2\,(W\, v_r^2 + p)\,\} + \frac{1}{r\,\sin\theta}\,\partial_\theta\,(\sin\theta\, W\, v_r\, v_\theta)$$
$$-\frac{W}{r}\,v_\theta^2 - \frac{2p}{r} = 0, \quad (2\cdot1\text{c})$$

$$\partial_t(W\, v_\theta) + \frac{1}{r}\,\partial_r\,(r\, W\, v_r\, v_\theta) + \frac{1}{r\,\sin\theta}\,\partial_\theta\,\{\sin\theta\,(W\, v_\theta^2 + p)\,\}$$
$$+\frac{2}{r}\,W\, v_r\, v_\theta - \frac{p}{r}\,\cot\theta = 0, \quad (2\cdot1\text{d})$$

where

$$D \equiv n\,\gamma, \quad\quad\quad\quad (2\cdot2)$$
$$W \equiv (e + p)\,\gamma^2 = 4p\gamma^2, \quad\quad\quad\quad (2\cdot3)$$

and n, e and p are the number density, energy density and pressure. We have assumed that after a strong shock, that the relativistic fluid is radiation dominated, i.e. $e = 3p$.

Blandford and McKee[7] obtained a spherically symmetric similarity solution of Eqs. (2·1a) – (2·1d). This solution can be written in terms of t and r. The

kinematical energy of the shock decreases with time. The Lorentz factor Γ of the shock front therefore indicates the timescale. In place of the radial coordinate, they introduced a new coordinate χ as the similarity variable. The position of the shock front corresponds to $\chi = 1$, and the interior region corresponds to $\chi > 1$. These new coordinates are mathematically defined as

$$\Gamma^2 = (t/t_0)^{-m}, \tag{2·4}$$

$$\chi = \{1 + 2\,(m+1)\,\Gamma^2\}\,(1 - r/t), \tag{2·5}$$

where t_0 is a constant, and the index m determines the energy supply rate of the blast wave. For the $m = 3$ case, the motion corresponds to an adiabatic point explosion, that is, an impulsive injection of energy at the center. For the case $m < 3$, the decrease of the velocity is less than that for the adiabatic case. This means that the solution corresponds to a blast wave with additional power supply. [7] This solution has additional inner shock and a contact discontinuity inside the flow.

　　We assume a strong shock, that is, that the kinematical shock energy is extremely large. This situation corresponds to a large value of Γ. The solution matched with the strong shock condition can be expressed by

$$D_0 = 2\,n_1\,\Gamma^2\,h \;, \tag{2·6}$$

$$p_0 = \frac{2}{3}\,w_1\,\Gamma^2\,f \;, \tag{2·7}$$

$$W_0 = \frac{4}{3}\,w_1\,\Gamma^4\,f\,g \;, \tag{2·8}$$

$$(v_{r0},\; v_{\theta 0}) = \left(1 - \frac{1}{\Gamma^2\,g},\; 0\right) \;, \tag{2·9}$$

$$\gamma^2 = \frac{1}{2}\,\Gamma^2\,g \;, \tag{2·10}$$

where n_1 and w_1 are the number density and enthalpy in front of the shock. Since we consider a strong shock, the external medium is cold and non-relativistic, and thus the pressure of the medium in front of the shock can be neglected. We also assume that the density n_1 varies as a power of the radius:

$$n_1 \propto r^{-k}. \tag{2·11}$$

The functions $f(\chi)$, $g(\chi)$ and $h(\chi)$ can be obtained by solving differential equations, but they reduce to simple analytic forms for the special case $m = 3 - k$ as

$$f = \chi^{-(4k-17)/(3k-12)}, \tag{2·12a}$$

$$g = \chi^{-1}, \tag{2·12b}$$

$$h = \chi^{-(2k-7)/(k-4)}. \tag{2·12c}$$

We only examine the stability of the case that includes the point explosion into the constant density $k = 0$. The calculation is simply, and the result is likely to be common to other cases, in which the growth/decay rate may be modified.

2.2.   *Perturbation equations*

We denote the Eulerian variation of a variable by δ, and we expand variables, e.g. the pressure as

$$p = p_0 + \delta p = p_0 \left\{ 1 + (\Gamma^2)^s \, \xi_P \, P_l \right\} , \qquad (2 \cdot 13)$$

where $P_l(\cos\theta)$ is the Legendre polynomial of order l, and a power law form is assumed with respect to the "time" Γ. Since the background quantities change in a self-similar way, the perturbations also have self-similar forms. The index s is a complex number in general. The real part of it represents the growth rate for $\Re(s) < 0$, since the factor Γ decreases with time. In a similar way, perturbations of the density and velocity are expanded as

$$D = D_0 + \delta D = D_0 \left\{ 1 + (\Gamma^2)^s \, \xi_D \, P_l \right\} , \qquad (2 \cdot 14)$$

$$v_r = v_{r0} + \delta v_r = 1 - \frac{1}{\Gamma^2 g} \left\{ 1 + (\Gamma^2)^s \, \xi_R \, P_l \right\} , \qquad (2 \cdot 15)$$

$$v_\theta = \delta v_{\theta 0} = (\Gamma^2)^s \, \xi_T \, \frac{d}{d\theta} P_l . \qquad (2 \cdot 16)$$

A perturbation of the function W can be expressed by the perturbations of the pressure and radial velocity as

$$W = W_0 + \delta W = W_0 \left\{ 1 + (\Gamma^2)^s \, g \, (2\,\xi_P + \xi_R) P_l \right\} . \qquad (2 \cdot 17)$$

Using the definitions in Eqs. (2·1a) – (2·1d), we have the linearized perturbation equations. After separating the time and angular parts, we have the differential equations for the functions ξ_D, ξ_P, ξ_R and ξ_T. The explicit forms can be written as

$$(k-4)\chi\frac{d\xi_D}{d\chi} - \frac{3}{2}(k-4)\chi\frac{d\xi_P}{d\chi} = (k-3)s\xi_D + \frac{4}{3}(k-2)\xi_R$$
$$-\frac{1}{2}\left\{-3(s+4)+k(s+6)\right\}\xi_P, \quad (2 \cdot 18a)$$

$$(k-4)\chi\frac{d\xi_R}{d\chi} + \frac{3}{2}(k-4)\chi\frac{d\xi_P}{d\chi} = -\left\{3s+\frac{5}{3}-k\left(s+\frac{1}{3}\right)\right\}\xi_R$$
$$+\frac{1}{2}\left\{3(s-4)-k(s-6)\right\}\xi_P, \quad (2 \cdot 18b)$$

$$(k-4)\chi\frac{d\xi_T}{d\chi} = -\left\{3s+\frac{14}{3}-k\left(s+\frac{7}{3}\right)\right\}\xi_T, \quad (2 \cdot 18c)$$

$$(k-4)\chi\frac{d\xi_D}{d\chi} + 2(k-4)\chi\frac{d\xi_R}{d\chi} = (k-3)s\xi_D - 2(3k-7)\xi_R$$
$$-l(l+1)\xi_T, \quad (2 \cdot 18d)$$

where we have retained the highest order of Γ only. The differential Equations (2·18a) – (2·18d) can be solved analytic ally. The solutions are expressed with four integration constants, a, b, c and d:

$$\xi_D = a\chi^{p_1} + bq_1\, l\,(l+1)\chi^{p_2} + cq_{4_-}\chi^{p_+} + dq_{4_+}\chi^{p_-}\ , \tag{2·19a}$$

$$\xi_R = bq_2\, l\,(l+1)\chi^{p_2} + cq_{5_+}\chi^{p_+} + dq_{5_-}\chi^{p_-}\ , \tag{2·19b}$$

$$\xi_P = bq_3\, l\,(l+1)\chi^{p_2} + c\chi^{p_+} + d\chi^{p_-}\ , \tag{2·19c}$$

$$\xi_T = b\chi^{p_2}\ . \tag{2·19d}$$

Here the indices p_i and coefficients q_i depend on s only:

$$p_1 = \frac{k-3}{k-4}\, s\ , \tag{2·20a}$$

$$p_2 = \frac{k(3s+7)-9s-14}{3(k-4)}\ , \tag{2·20b}$$

$$p_\pm = \frac{-k(6s+17)+18s+43 \pm f_1}{6(k-4)}\ , \tag{2·20c}$$

where

$$f_1 = \Big\{ k^2\left(48\,s^2 + 192\,s + 841\right) - 2\,k\left(144\,s^2 + 528\,s + 1943\right)$$
$$+432\,s^2 + 1440\,s + 4489 \Big\}^{1/2} \tag{2·21}$$

and

$$q_1 = -\Big[7\,(k-2)\Big\{2\,k^2\left(4\,s^2 + 23\,s + 5\right) - k\left(48\,s^2 + 240\,s + 43\right)$$
$$+72\,s^2 + 306\,s + 46\Big\}\Big]^{-1}\Big\{k^2\,(4\,s-2) - k\,(26\,s-5) + 42\,s - 2\Big\}\ , \tag{2·22a}$$

$$q_2 = -\Big\{2\,k^2\left(4\,s^2 + 23\,s + 5\right) - k\left(48\,s^2 + 240\,s + 43\right) + 72\,s^2 + 306\,s + 46\Big\}^{-1}$$
$$\times \Big\{k(4s+1) - 2(6s+1)\Big\}, \tag{2·22b}$$

$$q_3 = \Big\{2\,k^2\left(4\,s^2 + 23\,s + 5\right) - k\left(48\,s^2 + 240\,s + 43\right) + 72\,s^2 + 306\,s + 46\Big\}^{-1}$$
$$\times \Big\{2(2k-3)\Big\}, \tag{2·22c}$$

$$q_{4_\pm} = \Big[4\Big\{k\,(s+4) - 3\,s - 10\Big\}\Big\{k^2\left(4\,s^2 + 9\,s - 23\right) - k\left(24\,s^2 + 50\,s - 101\right)$$
$$+36\,s^2 + 69\,s - 110\Big\}\Big]^{-1}\Big[k^3\left(12\,s^3 + 113\,s^2 + 231\,s - 406\right)$$
$$-k^2\left(108\,s^3 + 949\,s^2 + 1822\,s - 2736\right) + k\left(324\,s^3 + 2643s^2 + 4763s - 6126\right)$$
$$-324\,s^3 - 2439\,s^2 - 4128\,s + 4556 \pm \Big\{k^2\left(s^2 + 3\,s - 14\right)$$
$$-k\left(6\,s^2 + 17\,s - 62\right) + 9\,s^2 + 24\,s - 68\Big\}f_1\Big], \tag{2·22d}$$

$$q_{5_\pm} = \Big[8\Big\{k\,(s+4) - 3\,s - 10\Big\}\Big]^{-1}\left(-29k + 67 \pm f_1\right). \tag{2·22e}$$

The physical interpretation of the solutions is evident. The term with the constant *a* simply represents the perturbation of the number density, without disturbing any

other quantities. The terms with the constant b represent the perturbation of the angular momentum. This mode is possible only for non-spherical perturbations ($l \neq 0$). For a spherically symmetric perturbation, $\xi_T = 0$, $l = 0$. In this case, the solution should be reduced by setting $b = 0$ in Eqs. (2·18a) – (2·18d). The terms involving the constants c and d represent the pressure waves propagating in the inward and outward directions.

2.3. *Regularity condition at the origin*

For the boundary condition at the origin, we require that the fluid does not undergo divergent perturbations. Also, the pressure perturbation should vanish: $\delta p \rightarrow 0$. This condition corresponds to

$$\xi_P \rightarrow 0 \tag{2·23}$$

for $\chi \rightarrow \infty$. It restricts the possible form of the power index $\Re(s)$; that is, ξ_P must decrease as the origin is approached. The explicit condition is written as

$$\Re(s) < \frac{7(k+2)}{3(k-3)}. \tag{2·24}$$

2.4. *Boundary conditions at the shock front*

Here we consider the deformation of an expanding shock wave. The radius of the shock is assumed to be given by

$$r = t\left\{1 - \frac{1}{2(m+1)\Gamma^2}\right\} + \eta, \tag{2·25}$$

where the first term denotes the radius of the unperturbed shock and the second denotes the perturbation. We also assume that the perturbation function has the power-law form

$$\eta = -\frac{\alpha}{2} t \left(\Gamma^2\right)^{s-1} P_l , \tag{2·26}$$

where α is the normalization factor. This change of the shock front induces a radial velocity as

$$\delta V_r = \frac{d\eta}{dt} = -\alpha \frac{4 - 3s}{2} \left(\Gamma^2\right)^{s-1} P_l . \tag{2·27}$$

We now apply the jump condition for the perturbation functions at this perturbed shock front. That is, we stipulate that the number flux, energy flux and momentum flux be continuous across the surface (see A). The values at the perturbed position are evaluated by the Lagrange perturbation. For example, the pressure at the perturbed shock position is given by

$$\Delta p = \delta p + \eta \frac{\partial p_0}{\partial r} . \tag{2·28}$$

It is also easy to rewrite the boundary conditions at shock front as

$$\xi_D/\alpha = 21s - 10k + 13, \tag{2·29a}$$
$$\xi_P/\alpha = 9s - 4k + 5, \tag{2·29b}$$
$$\xi_R/\alpha = 12s - 5k + 5. \tag{2·29c}$$
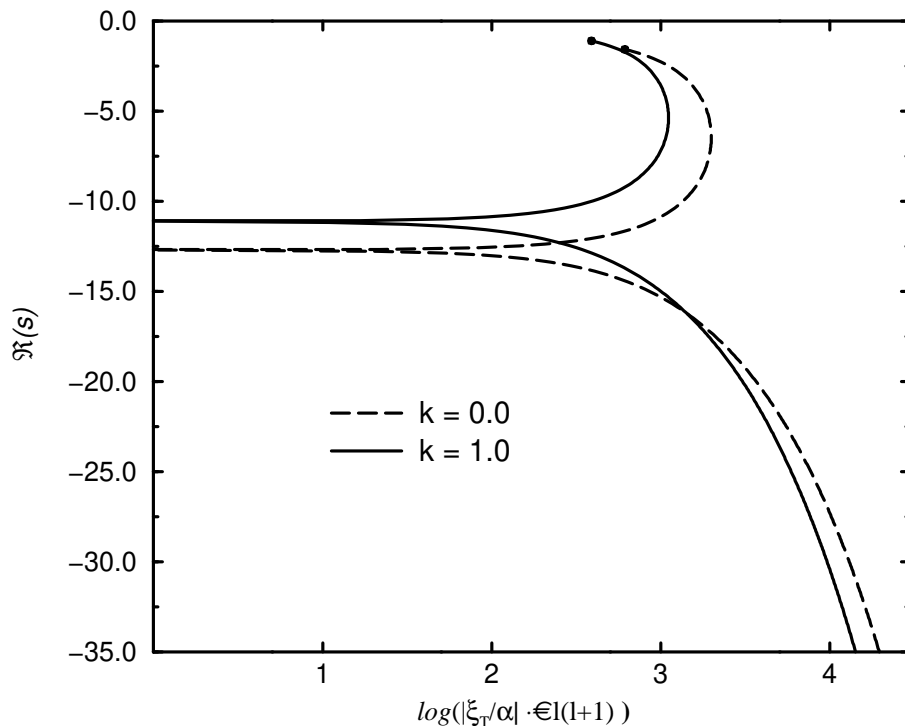
2.5. *Approximate solution*

Fig. 1. The growth rate as a function of normalized tangential velocity, $|\xi_T/\alpha| \cdot l(l+1)$. Two curves are shown corresponding to the external density distribution k. Uniform case is $k = 0$. Dots near $\Re(s) = -1.5$ are the maximum values which are determined from the regularity condition at the origin.

We can easily determine the integration constants by matching the jump conditions to the interior solution Eqs. (2·19a) – (2·19d) (see B). The temporal dependence s is specified by one parameter, the velocity in the tangential direction. We use the normalized value $|\xi_T/\alpha| \cdot l(l+1)$ and plot the growth rate $\Re(s)$ as a function of it in Fig. 1. Both the cases $\xi_T/\alpha < 0$ and $\xi_T/\alpha > 0$ are shown. For the spherically symmetric case $\xi_T/\alpha \cdot l(l+1) = 0$, the growth rate is $\Re(s) \sim -12.7$ for $k = 0$. As the value ξ_T/α decreases, $\Re(s)$ increases. We only show the region of $\Re(s)$ limited by Eq. (2·24); that is, the curves are terminated near $\Re(s) = -1.5$. As the value ξ_T/α increases from zero, $\Re(s)$ monotonically decreases. This implies that the temporal behavior depends significantly on the Γ factor. The mode grows strongly with the deceleration of the background fluid. In particular, the growth rate is large for shorter wavelengths in the tangential direction. In this figure, we also show the effect of the external density gradient, uniform ($k = 0$) and a decreasing slope with the radius ($k = 1$). The general features of the growth rate do not depend on the density distribution. The growth rate is modified by about 10%.

The radial functions of the background and perturbation fields are shown in Fig. 2. We display the density profiles near the shock front, which corresponds to
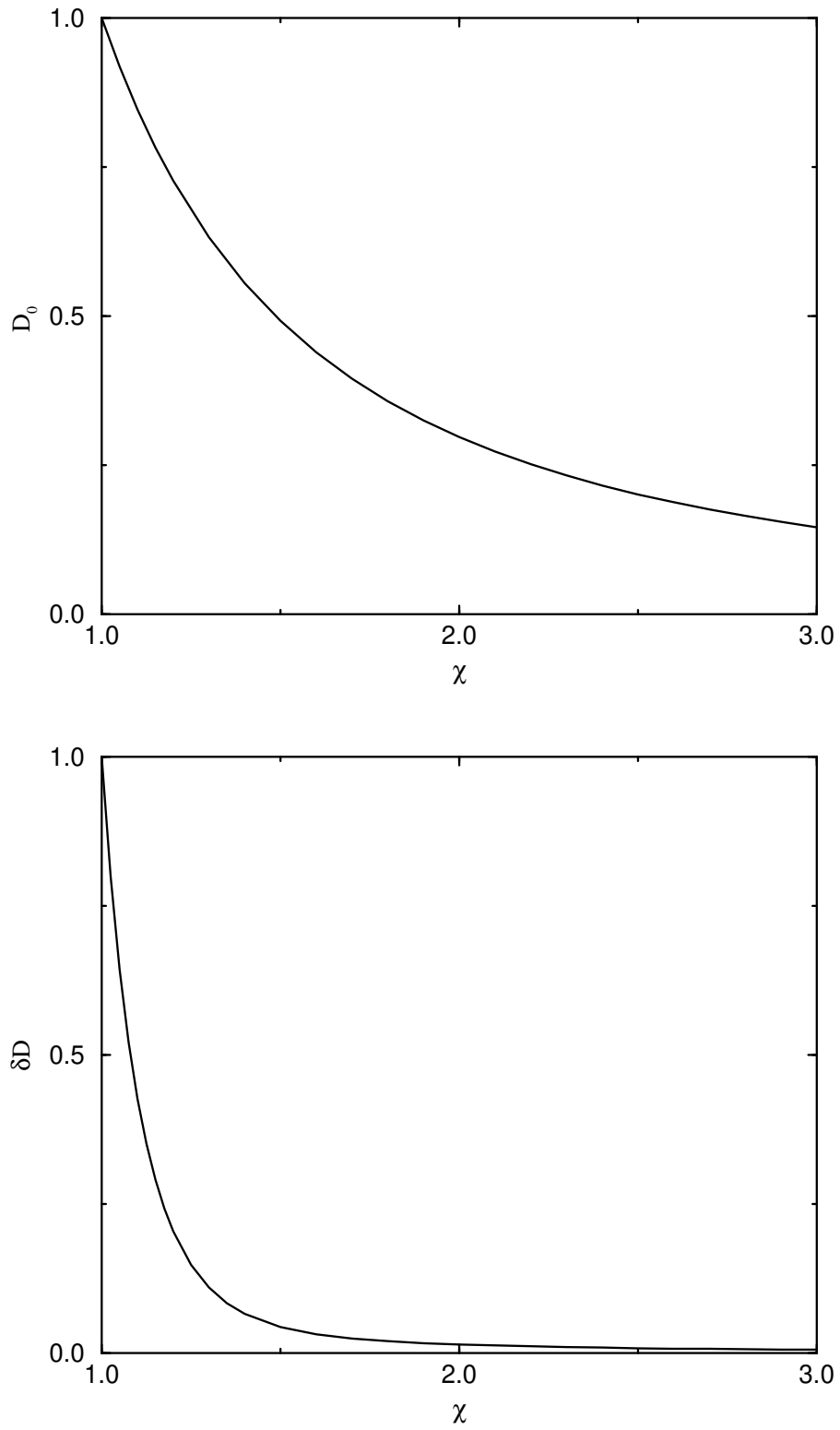
J. Ogura and Y. Kojima

Fig. 2. The shape of background density(D_0) and its perturbation value(δD) normalized at shock front. The parameters adopted here are $Bl(l+1) = 1000$ and $k = 0$. χ is a similarity variable which show the distance from shock front, where $\chi = 1$ is the shock front.

$\chi = 1$. The thickness of the expanding shell is approximated by the region from $\chi = 1$ to 2. The radial function of the perturbation is localized within the small region of the shell; that is, it is a quite steep function.

§3.   Summary and discussion

In this paper, we have studied the linear stability of a spherically expanding shock in the ultra-relativistic limit, i.e. the large Γ limit. The temporal behavior of the perturbation is expressed by a power law in Γ. We found a solution that grows with the deceleration of the shock. The growth rate becomes large for short wavelengths of the angular fluctuation. That is, there exists a rapidly growing mode for the non-spherically symmetric displacement. Vishniac[11] discussed the physical interpretation of the unstable mode in the non-relativistic blast wave. It is important to remember that two kinds of pressures exerted to the shock plane have completely different natures. In the exterior region before the shock, the ram pressure dominates and is parallel to the direction of the shock propagation. After the shock, the thermal pressure dominates and is isotropic. When the shock spherically expands, two directions, i.e. the direction of the propagation and the normal direction of the plane coincide. However, when the shock is rippled with the tangential velocity, two pressures lose the balance in the tangential direction. This unbalance is expected to be larger with the increase of the velocity. The unstable mechanism indeed works in the ultra relativistic blast wave as shown in this paper. This result depends on several assumptions and approximations, but it is quite suggestive. Suppose, e.g., for the relativistic flow dynamics from $\Gamma = 10^2$ to 1 associated with the gamma-ray bursts, that the amplitude increases by more than a factor of 10^{20}. The dominant scale of the unstable mode depends on both the initial disturbance and the growth rate. If there is no characteristic wavelength in the initial stage of the expansion, the unstable mode is likely to be non-linear at the smaller scale due to the large growth rate. This mode may lead to a number of fragmentations. The radiation from the blobs may be reflected by an irregular time-profile of the gamma-rays.

In order to check this possibility, further study is necessary. For dynamical evolution, we must simulate relativistic flows using axi-symmetric or 3-dimensional numerical codes. Fluctuations are manifest only in the small region after the shock front. The structure may be found only by using a fine resolution in the numerical calculations. The unstable mode may be suppressed to a certain value of the amplitude. Also, the size and number relations of the fragmentation can be estimated. The effect of the flow dynamics will appear in the emission, but the gamma-ray emission process is not clear at moment. However, the complex structure of the shock front may universally give the time history of the burst, irrespective of the detailed behavior of the emission process.

Appendix A
—— *Jump Conditions* ——

The difference between the values on the two sides of a surface is denoted by $[a] \equiv a_1 - a_2$, where the subscript "1" indicates the fluid located before the shock wave, and "2" after the shock wave. The number density and energy-momentum are continuous across the shock surface. The jump conditions for the relativistic adiabatic shock are given by

$$[n\, u^\mu\, N_{s\mu}] = 0 \ , \tag{A·1}$$

$$[T^{\mu\nu}\, N_{s\mu}\, N_{s\nu}] = 0 \ , \tag{A·2}$$

$$[T^{\mu\nu}\, N_{s\mu}\, U_{s\nu}] = 0 \ , \tag{A·3}$$

where $T^{\mu\nu}$ and u^μ are the energy-momentum tensor and the 4-velocity of the fluid. The time-like unit vector $N_{s\mu}$ describes the motion of the shock front, and the space-like unit vector $U_{s\mu}$ describes the normal direction of the surface. For a spherically expanding shock wave, they are given by $N_{s\mu} = \{\Gamma V, \Gamma, 0\}$ and $U_{s\mu} = \{\Gamma, \Gamma V, 0\}$. We consider linear perturbations of them. The explicit forms are given by

$$N_{s\mu} = \left\{ \Gamma\left(V + \Gamma^2\, \delta V_r\right), \Gamma\left(1 + V\,\Gamma^2\, \delta V_r\right), N_\perp \right\} , \tag{A·4}$$

$$U_{s\mu} = \left\{ \Gamma\left(1 + V\,\Gamma^2\, \delta V_r\right), \Gamma\left(V + \Gamma^2\, \delta V_r\right), U_\perp \right\} , \tag{A·5}$$

where δV_r is the velocity perturbation in the radial direction, and $N_\perp$ and $U_\perp$ are the tangential components of the perturbation of the variables. Their explicit forms are not necessary in the calculations.

Appendix B
—— *Analytic Solution* ——

The coefficients of the analytic solutions Eqs. (2·19a) – (2·19d) are determined as

$$
\begin{aligned}
a = \Big[& 28\,(k-2)\left\{ k\,(4s-5) - 12\,s + 7 \right\} \\
& \times \left\{ k^2\left(4\,s^2 + 9\,s - 23\right) - k\left(24\,s^2 + 50\,s - 101\right) + 36\,s^2 + 69\,s - 110 \right\} \Big]^{-1} \\
& \times \Big[-8\,k^5\left(352\,s^3 - 584\,s^2 - 3983\,s + 5905\right) \\
& + k^4\left(5616\,s^4 + 22872\,s^3 - 115057\,s^2 - 225180\,s + 425829\right) \\
& - k^3\left(60624\,s^4 + 56344\,s^3 - 794477\,s^2 - 518881\,s + 1515622\right) \\
& + k^2\left(242352\,s^4 + 11088\,s^3 - 2362877\,s^2 - 277212\,s + 2660875\right) \\
& - k\left(423792\,s^4 - 125064\,s^3 - 3211707\,s^2 + 457097\,s + 2302554\right) \\
& + 2\left(136080\,s^4 - 61020\,s^3 - 817893\,s^2 + 227748\,s + 392500\right)
\end{aligned}
$$

$$-3\left\{8\,k^4\left(6\,s^2-s-15\right)-k^3\left(108\,s^3+451\,s^2-420\,s-867\right)\right.$$
$$+k^2\left(900\,s^3+1418\,s^2-2409\,s-2273\right)$$
$$-k\left(2484\,s^3+1605\,s^2-4737\,s-2558\right)$$
$$\left.+2268\,s^3+342\,s^2-3060\,s-1040\right\}f_1\Bigg]\ ,\qquad\text{(B·1a)}$$

$$b=\left[4\,l(l+1)\left\{k\,(4\,s-5)-12\,s+7\right\}\right]^{-1}$$
$$\times\left[8\,k^3\left(20\,s^2+155\,s-38\right)-k^2\left(384\,s^3+4012\,s^2+7249\,s-1265\right)\right.$$
$$+k\left(2304\,s^3+17844\,s^2+13577\,s-1539\right)$$
$$-18\left(192\,s^3+1208\,s^2+439\,s-30\right)-\left\{8\,k^2\,(2\,s+3)\right.$$
$$\left.\left.-k\left(36\,s^2+125\,s+63\right)+2(54\,s^2+75\,s+20)\right\}f_1\right]\ ,\qquad\text{(B·1b)}$$

$$c=\left[2\left\{7-12\,s+k\,(-5+4\,s)\right\}\left\{2\,k^2\left(4\,s^2+23\,s+5\right)\right.\right.$$
$$\left.\left.-k\left(48\,s^2+240\,s+43\right)+72\,s^2+306\,s+46\right\}\right]^{-1}$$
$$\times\left[\left\{8\,k^2\,(2\,s+3)-k\left(36\,s^2+125\,s+63\right)+108\,s^2+150\,s+40\right\}\right.$$
$$\times\left\{-2\,k^2\left(8\,s^2+34\,s-21\right)+k\left(96\,s^2+372\,s-149\right)\right.$$
$$\left.\left.-144\,s^2-504\,s+121+(2\,k-3)f_1\right\}\right],\qquad\text{(B·1c)}$$

$$d=0.\qquad\text{(B·1d)}$$

References

[1] E. Costa, et al., Nature. **387** (1997), 783.
[2] C. Akerlof, et al., Nature. **398** (1999), 400.
[3] A.J. Castro-Tirado, et al., preprint (astro-ph/9811455).
[4] E. Waxman, Astrophys.J. **485** (1997a), L5.
[5] E. Waxman, Astrophys.J. **489** (1997b), L33.
[6] R. Sari, and T. Piran, Astrophys.J. **485** (1997), 270.
[7] R.D. Blandford, and C.F. McKee, Phys. of Fluids **19** (1976), 1130.
[8] S. Kobayashi, T. Piran, and R. Sari, preprint (astro-ph/9803217).
[9] D. Ryu, and E.T. Vishiniac, Astrophys.J. **313** (1987), 820.
[10] J. Goodman, Astrophys.J. **308** (1986), L47.
[11] E.T. Vishniac, Astrophys.J. **274** (1983), 152.